JOURNAL OF MATERIALS SCIENCE 27 (1992) 2549–2555

Characterization of TiO_2 and ZrO_2 coatings on silica slabs and fibres

K. JUREK*, M. GUGLIELMI‡, G. KUNCOVÁ§, O. RENNER*, F. LUKEŠ¶, M. NAVRÁTIL¶, E. KROUSKÝ*, V. VORLÍČEK*, K. KOKEŠOVA*
* *Institute of Physics, Czechoslovak Academy of Sciences, Cukrovarnická 10, 160 00 Prague 6, Czechoslovakia*
‡ *Dipartimento di Ingegneria Meccanica, Sez. Materiali, Via Marzolo 9, 35100 Padova, Italy*
§ *Institute of Chemical Process Fundamentals, Czechoslovak Academy of Sciences, 165 02 Prague 6, Czechoslovakia*
¶ *Department of Solid State Physics, Masaryk University, Kotlářská 2, Brno, Czechoslovakia*

Titanium and zirconium dioxide coatings were deposited on optical fibres by the sol–gel procedure. The thickness of the layers on fibres was established by measurement of the intensity of characteristic X-rays by an electron microprobe analyser. The accuracy of the measurements was verified on broken layers by scanning electron microscopy. Also determined were the thicknesses of similar layers deposited on flat silica substrates with an ellipsometer and stylus surfometer as well as from reflectivity spectra and from specular total reflection of X-rays. The densities of TiO_2 and ZrO_2 layers on silica glass slabs were determined by X-ray total reflection. Values of 3.16 ± 0.02 and 4.69 ± 0.03 gm cm^{-2} were found for titania and zirconia, respectively. The crystallinity of layers on silica plates was investigated by Raman spectroscopy. The thicknesses of coatings prepared by the dipping technique were related to the withdrawal speed. Equations for Newtonian and non-Newtonian fluids were tested and compared. A pseudo-plastic behaviour was suggested for all the solutions used in the experiments.

1. Introduction

A coating on glass changes the optical, chemical, mechanical and electrical properties of its surface. Changing the quality of optical fibre surfaces is used for the protection of fibres and may also be used to create new optical fibre sensors. The best known and most widely used protection of optical fibres is coating by organic polymers. Primary protection with metals is also known. Both methods are used for the formation of a hermetically sealed jacket and for the creation of an electrically conductive layer. An alternative is ceramic primary protection, which can be realized by a number of techniques (application of suspensions, magnetron sputtering, pyrolytic decomposition, etc.) [1, 2]. The main disadvantages of organic polymers are that they cannot protect the fibre against air moisture and they limit the temperature region of fibre applicability to 350 °C. The main drawback of fibre metallic jackets is the large difference between the coefficients of thermal expansion of the metal and the fibre: this results in cracking of the metallic layer and its fast corrosion due to air moisture. A disadvantage of ceramic protection is the sputtering equipment, which is often very complicated and expensive.

The sol–gel method could be an interesting alternative for the deposition of ceramic coatings. It was recently shown that optical fibres may be coated by the sol–gel method during the drawing process, using a soft nozzle filled with an appropriate solution through which the fibre is drawn [3].

The characterization of layers on fibres is complicated by the curvature of their surface. The commonly used methods for the measurement of film thickness – ellipsometry, stylus or optical reflectance – cannot be used. Direct microscopic measurement on the polished cross-section of fibres is difficult because of the difficulty in the preparation of a good-quality cross-section, and gives only very localized information. Nevertheless, in the case of thick cracked layers it is possible to measure their thickness in the scanning electron microscope.

In this work the thicknesses of oxide layers were evaluated by measuring characteristic X-ray intensities of elements contained in the layer using electron probe micro analysis (EPMA). To determine the thickness by this method the dependence of generated X-ray intensity on the film thickness needs to be determined. The necessary condition is that the depth of penetration of primary electrons under the surface of the specimen exceeds the thickness of the measured layer. An appropriate calibration curve can be obtained experimentally by using a set of suitable well-defined thin film standards of the same material

0022–2461

deposited on the same substrate. A second more general method is the theoretical calculation of the characteristic X-ray intensity versus film thickness [4]. When evaluating the experimental results, other macroscopic parameters of the layers must be taken into account. In particular, the role of density might be crucial. Therefore, the layers were also studied from this point of view, performing density measurements by total reflection of X-rays.

In this work the influence of surface curvature of substrates on the dip-coating process is also studied by analysing the thickness values of films deposited on fibres of different radii. Some suggestions are also presented of a possible non-Newtonian behaviour of sol–gel solutions.

2. Experimental procedure

2.1. Preparation of samples

The solutions used in this work are described in Table I. The reagents were mixed and allowed to react under stirring for 0.5 h. The solutions were kept in closed plastic bottles in a refrigerator until required.

Before being used the solutions were centrifuged and successively filtered through Millipore filters of 0.22 μm pore size in order to eliminate dust or aggregates formed during storage.

Silica fibres of three different diameters (125, 200 and 350 μm) drawn from Herasil rods were cleaned by wiping with an ethanol-soaked tissue and dried. Coatings were deposited by dipping 10 cm long specimens in solutions A, B, C and D (Table I) with vertical withdrawal speeds of 2.5, 19 and 32 cm min^{-1} in a chamber where relative humidity and temperature were maintained constant at 63–66% and 28–30 °C, respectively. The coated fibres were then heat treated at 200, 400 and 800 °C for 3 min, in order to investigate the changes in layers upon fast thermal treatment (simulating processes during on-line coating [3]).

Coatings of the same type were also deposited on flat silica samples obtained from Herasil rod. In this case the coated samples were treated only at 500 °C for 3 min. Flat specimens having different thicknesses of TiO_2 and ZrO_2 coatings were denoted Ti1, Ti2, Ti3, Ti4 (Tix) and Zr1, Zr2, Zr3 and Zr4 (Zrx), respectively. The Zr4 sample was obtained by double dipping.

TABLE I Composition of solutions

Solution	Alkoxide (g)	Solvent (ml)	H_2O (ml)	acac (ml)	HCl (ml)
A	$Ti(n\text{-}OBu)_4$ 100	nBuOH 13.5	10.6	24	–
B	$Ti(i\text{-}OPr)_4$ 100	iPrOH 19.0	17.7	31	Conc. 15
C	$Zr(n\text{-}OBu)_4$[a] 100	nBuOH 27.6	33.6	24	1 N 7
D	$Zr(n\text{-}OBu)_4$ 100	nBuOH 16.0	39.0	27	1 N 4

[a] Zr(n-OBu) + nBuOH complex, 28% ZrO_2 (Ventron).

2.2. Characterization of samples

The thicknesses of oxide layers on Tix and Zrx samples were both measured by several different techniques: EPMA, ellipsometry, optical reflection, X-ray total reflection and stylus measurements. These methods also provided other information. In particular it was possible to determine the refractive index by ellipsometry and the optical spectral reflectance and density by the X-ray total reflection method. Raman measurements were also performed to obtain some structural information. The thicknesses of coatings deposited on fibres were measured by EPMA.

2.2.1. Thickness measurement by EPMA

A Jeol JXA-733 X-ray microanalyser was used. Intensities of TiK_{α_1} and ZrL_{α_1} lines were measured using a wavelength-dispersive spectrometer with a PET crystal at an energy of primary electrons of 25 keV. Polished single crystals of rutile and zirconium were used as standards.

Glass fibres were fixed on a brass stage and covered with a carbon layer. Knowing that the minimum fibre diameter was 125 μm, the effect of surface curvature on measured intensity was tested. Fibres were placed horizontally and the vertical beam was pointed first at the highest position of the perimeter and then shifted $\pm$ 10 μm and $\pm$ 20 μm apart. The variation of X-ray intensity did not exceed 5% in all cases. The possible error in the intensity measurement due to the fibre–spectrometer orientation was also tested by rotating the fibre in the range 0–360°. The intensity remained constant within 3%. For layers treated below 400 °C it was impossible to repeat the measurement on the same spot, due to the damage caused by the electron beam.

The determination of the film thickness by EPMA is based on the fact that if the penetration depth of primary electrons is greater than the thickness of the layer, the intensity of characteristic X-rays emitted from the layer depends not only on the chemical composition but also on its thickness. This condition is generally fulfilled for submicrometre layers using primary electron energies higher than about 20 keV.

However, common calculations converting intensities to elemental composition can only deal with integral intensities emitted from bulk (infinitely thick) specimens. A Monte Carlo algorithm, on the other hand, can model the scattering and energy loss of primary electrons and consequent emission of X-rays in small steps (thus simulating the true process), so that the interface between the layer and substrate can be taken into account. In such a way it is possible to calculate emitted intensities for layers of various thicknesses, which enables a calibration curve to be drawn. In our program described elsewhere [5] multiple scattering theory was used.

Generally the penetration of primary electrons through the specimen is inversely proportional to the mass density (number of atoms per unit volume), so that the mass thickness of the layer can be actually determined. To calculate the geometrical thickness the density needs to be known. It is known that density

changes during the heat treatment due to a densification process of the gel. However, the density was only measured by the X-ray total reflection method for flat samples treated for 3 min at 500 °C. Thus thicknesses obtained on fibres treated at different temperatures are not the true thicknesses but numbers directly related to the mass thicknesses. This means that the same sample treated at different temperatures should exhibit the same value, provided that no mass loss occurs due to heating. Fortunately thick layers on fibres (dip-coated) heated to 400 and 800 °C exhibited cracks which enabled the film thickness to be measured directly by a scanning electron microscope (Fig. 1). The calculated thicknesses from EPMA measurement agreed with the values measured by SEM in the range ± 15%. Similar agreement was observed for on-line coated fibres in cases where the layers did not contain residues of organic compounds. After the critical loss of the organic parts of the layers, the densities of both the TiO_2 and ZrO_2 layers increased only slowly during heat treatment.

2.2.2. Ellipsometry

A Gaertner L119 ellipsometer with an He–Ne laser (λ = 632.8 nm) was used. The ellipsometric angles ψ and Δ were determined at four angles of incidence within the interval from 45 to 75° [6]. It was assumed that the systems studied could be represented by the model of non-absorbing substrate–non-absorbing film with flat boundaries, both isotropic and homogeneous. The experimental results were evaluated by the least-squares method.

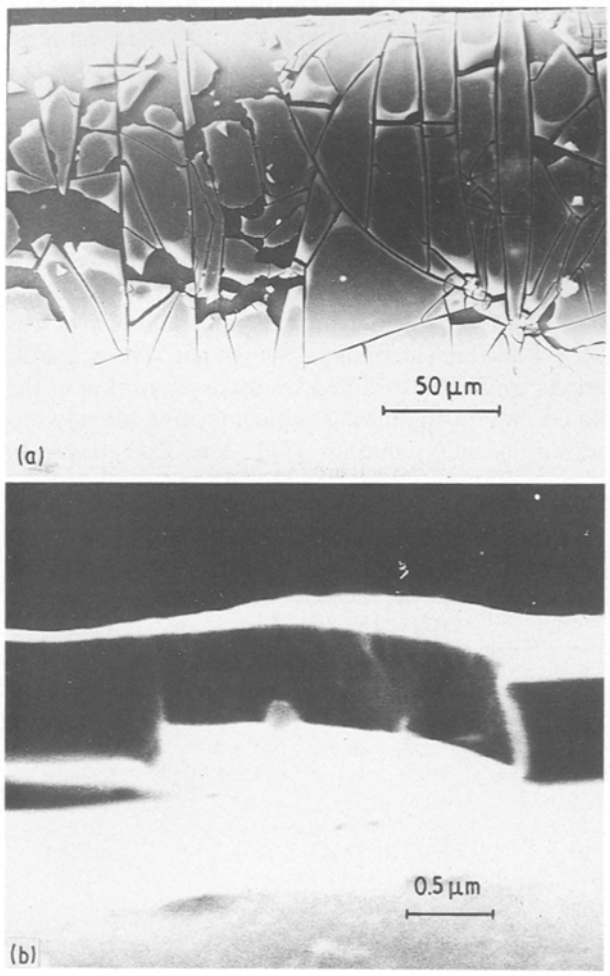

Figure 1 Scanning electron micrograph of a silica fibre coated with a thick ZrO_2 layer heated at 400 °C: (a) cracked layer, (b) sample in position for measurement of layer thickness.

2.2.3. Optical reflectance

The measurement of reflectance was carried out with a Zeiss SPM-1 spectrophotometer between 250 and 1000 nm by a point-to-point procedure. A slice of silicon single crystal with a perfectly smooth surface was used as a reflectance standard. The relative error $\Delta R/R$ of the reflectance measurement was between 0.01 and 0.03, depending on the absolute value of reflectance and on the spectral region used. Again, thin ZrO_2 and TiO_2 films were assumed to be non-absorbing materials. The thickness and the spectral dependence of refractive index were determined from the reflectance of a thin-film–substrate system. The refractive index and thickness were evaluated from the absolute value and the position of an extremium with odd interference order in the spectral dependence of reflectance. The standard deviation of thickness values was also determined. Further, the values of refractive index in the above region were evaluated from the measured reflectance curve, taking into account the errors in reflectance and thickness.

The refractive index values n_1 were approximated by the relation

$$n_1 = A + \frac{B}{\lambda^2} + \frac{B}{\lambda^4}$$

for both thin films.

2.2.4. X-ray total reflection

The densities of TiO_2 and ZrO_2 layers on flat silica samples were determined by the X-ray external total reflection method [7]. The shape of the reflection curve, i.e. the dependence of reflection coefficient of monochromatic X-ray radiation on incident glancing angle, is given by the chemical composition, density and thickness of the substrate and the surface layers under investigation. The determination of both latter parameters is based on the proportionality of the electron density to the refractive index decrements, which define the critical angle of total reflection, and the appearance of X-ray interference fringes at glancing angles just below the critical angle. The experimental curves were compared with the theoretical ones computed for different surface structures; the required parameters follow from the best-fit model.

The planarity of rectangular silica glass substrates with an area of about 1 cm^2 was checked in the dispersive and non-dispersive configuration of a double-crystal spectrometer. The CuK_{α_1} radiation from a microfocus X-ray tube was monochromatized and collimated by two Ge (3 3 3) analysing crystals with the measured sample situated between them. The intensity of reflected radiation was detected using a proportional counter; another counter monitored the

stability of the X-ray source. The reflection curves were measured stepwise with a minimum angular difference of 1.5×10^{-2} mrad in the region of the critical angle.

2.2.5. Stylus measurements

Film thicknesses were also measured by an Alpha-Step 200 (Tencor Instruments) stylus apparatus. Small grooves were produced with a sharp tool in several zones of each flat sample by scratching through the thickness of the gel layer after drying and before the final heat treatment.

2.2.6. Raman spectroscopy

Raman spectra were obtained at room temperature. The exciting laser beam (the 514.5 nm line of an Ar^+ laser) impinged on the sample either perpendicularly (backscattering geometry) or almost tangentially (close to the right-angle geometry). The second geometry appeared to be necessary to eliminate the strong signal originating in the substrate. The nominal incident power (monitored at the output from the laser head) was kept at 50 mW. The scattered light was analysed with a double-grating spectrometer (Spex 14018) and detected by a photomultiplier (RCA C31034) operating in the standard photon-counting mode. The spectral resolution was better than 4 cm^{-1}, and the error in the determination of frequencies of the Raman peaks did not exceed 2 cm^{-1}.

3. Results and discussion

A summary of the results, in terms of thickness, refractive index and density, obtained on Tix and Zrx samples is reported in Table II.

3.1. Coatings on flat samples

As may be observed in Table II, both types of coating, TiO_2 and ZrO_2, exhibited density and refractive index values lower than those reported for the known modifications of the corresponding crystalline phases. Mass densities stated for TiO_2 are 3.84 g cm^{-3} for anatase, 4.26 g cm^{-3} for rutile and 4.17 g cm^{-3} for brookite, while we found the value of 3.16 ± 0.02 g cm^{-3}. The optical refractive indices measured at $\lambda = 632.8$ nm are 2.5 for anatase and $n_0 = 2.58$, $n_e = 2.88$ for rutile, instead of 2.21 to 2.24 measured in this work. Monoclinic and tetragonal zirconia have density values of 5.56 and 6.10 g cm^{-3}, respectively, both higher than 4.69 found for the sol–gel layer.

It is known that sol–gel layers densify with increasing temperature and time, sometimes requiring temperatures much higher than 500 °C for complete densification. The heat treatment of coatings on flat samples, limited to 3 min at 500 °C, was sufficient to reach 80% of theoretical density in both titania and zirconia layers. As far as the structure is concerned, X-ray diffraction did not give unambiguous results for the crystallinity of the coatings. All the observed Raman frequencies are characteristic of the anatase phase [8–10], but the complete absence of rutile or amorphous phase is uncertain because these phases have frequencies which fall into the region where strong maxima originating in the substrate occur [9].

The determination of the layer thickness was performed by different methods, and the results compared. Table II shows that there was reasonable agreement among all determinations.

The optical methods of thickness determination differ in sensitivity depending on the quality of the substrate and the structure of the layer. Also related to the structure and homogeneity of the coating is the reliability of ellipsometric results, while the most sensitive to the planarity of the substrate is probably the X-ray total reflection method. The accuracy of reflectance thickness measurement in the case of Ti4 and Zr4 samples is rather low; neither film thickness nor refractive index could be evaluated by ellipsometry with reasonable accuracy, probably due to inhomogeneity of the coatings. Undulations were observed in the TiO_2 layer (Fig. 2), which were measured by EPMA: the thickness in the maxima of waves was 96 ± 4 nm and in minima 80 ± 4 nm. These undulations could be attributed to phase separation in the liquid film during drying, a phenomenon already observed in SiO_2 coatings [11]. The ZrO_2 layer in sample Zr4 was smooth, but it was prepared by

TABLE II Film thickness, refractive index ($\lambda = 632.8$ nm) and density of TiO_2 and ZrO_2 coatings on flat samples after heat treatment (3 min at 500 °C)

Measurement	TiO_2				ZrO_2			
	Ti1	Ti2	Ti3	Ti4	Zr1	Zr2	Zr3	Zr4
Thickness (nm) by:								
Stylus	116 ± 1	47 ± 1	102 ± 4	94	67 ± 2	46 ± 2	65 ± 2	117
Ellipsometry	–	44.3 ± 1.1	98.0 ± 0.3	[a]	–	–	74.2 ± 0.2	[a]
Reflectance	–	–	–	90 ± 12	–	–	–	121 ± 7
X-ray total reflection	–	–	–	88 ± 1.5	–	–	–	120 ± 2
EPMA	105 ± 2	40 ± 2	97 ± 2	91 ± 7	65 ± 2	39 ± 1	61 ± 2	105 ± 2
Refractive index by:								
Ellipsometry	–	2.244 ± 0.015	2.230 ± 0.011	[a]	–	–	1.941 ± 0.03	[a]
Reflectance	–	–	–	2.21 ± 0.05	–	–	–	1.98 ± 0.01
Density by:								
X-ray total reflection	–	–	–	3.16 ± 0.02	–	–	–	4.69 ± 0.03

[a] The accuracy of ellipsometric measurements was very low probably because of inhomogeneities in the coatings.

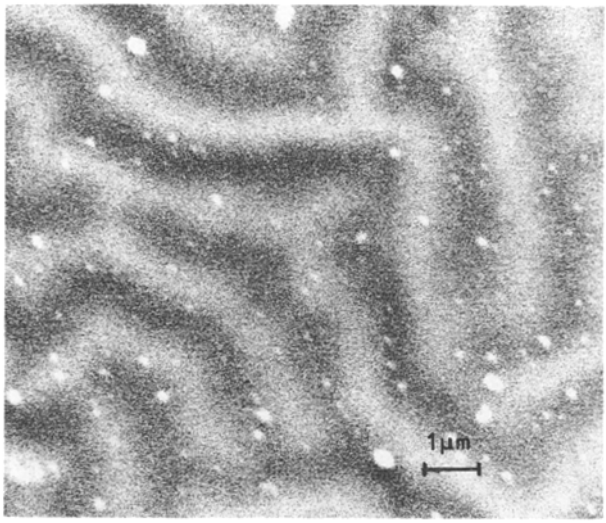

Figure 2 Scanning electron micrograph of Ti4 sample, showing waves in the coating.

double dipping. The layer was 42 ± 2 nm thick after the first dipping and 110 ± 4 nm after the second one (measured by EPMA). A thin layer of different composition (or a discontinuity) was probably created at the interface, which was detected by ellipsometry and X-ray total reflection but not by EPMA.

3.2. Coatings on fibre samples

The influence of various parameters on the thickness of dip-coated flat samples has been investigated by many authors [12–15] and acceptable agreements with hydrodynamic theories have been found. Theories have also been developed for the coating of filaments. It has been shown [16] that for thin wires, the Goucher number for which ($N_{Go} = R(\rho g/2\sigma)^{1/2}) \rightarrow 0$, the thickness of the layer reduces to a function of capillary number N_{Ca}:

$$\frac{h}{R} = \frac{1.33 N_{Ca}^{2/3}}{1 - 1.33 N_{Ca}^{2/3}} \quad (1)$$

where $N_{Ca} = V\mu/\sigma$, R is the filament radius, V is the withdrawal speed, μ, ρ and σ are the viscosity, density and surface tension of the coating solution, g is the acceleration due to gravity and h is the liquid film thickness. For very thin layers $R \gg h$ and the above equation can be reduced to the form

$$h = 1.33(\mu/\sigma)^{2/3} V^{2/3} R \quad (2)$$

If coatings are performed with a solution with constant physical properties and at constant V, the liquid film thickness h and also the solid film thickness t (assuming constant shrinkage and no mass loss during heating) are in direct proportion to fibre radius:

$$t = KR \quad (3)$$

The thickness of coatings on fibre samples was measured by EPMA as described in section 2.2.1. Three kinds of silica fibre, characterized by different radii (62.5, 100 and 175 μm), were coated by solutions A, B, C and D using different withdrawal speeds and treated at different temperatures. The measured values of thickness are shown as a function of fibre radius in Figs 3 and 4. The coating conditions are described in the legend. The comparatively large spread of measured values may be explained by the presence of cracks in the layers and by density fluctuations resulting in surface waves. It can be observed that the film thickness measured by EPMA is independent of temperature. As previously explained, the thickness values reported in Figs 3 and 4 are not the geometrical thicknesses, but are instead related to the mass thicknesses. The observed independence of temperature simply means that no significant mass loss occurred during heat treatment. By assuming that the density of layers on fibres heated above 400 °C was the same as that of the layers on slabs, it was possible to calculate

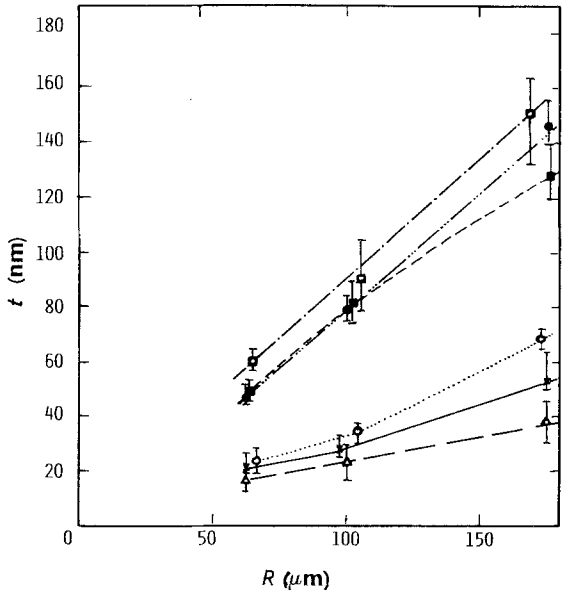

Figure 3 TiO_2 coatings on fibres: thickness versus fibre radius. Coating solution, temperature (°C) and V (cm min^{-1}) as follows: (○) A, 800, 2.5; (■) B, 200, 19; (×) A, 400, 2.5; (△) B, 800, 2.5; (●) B, 800, 19; (□) A, 800, 32.

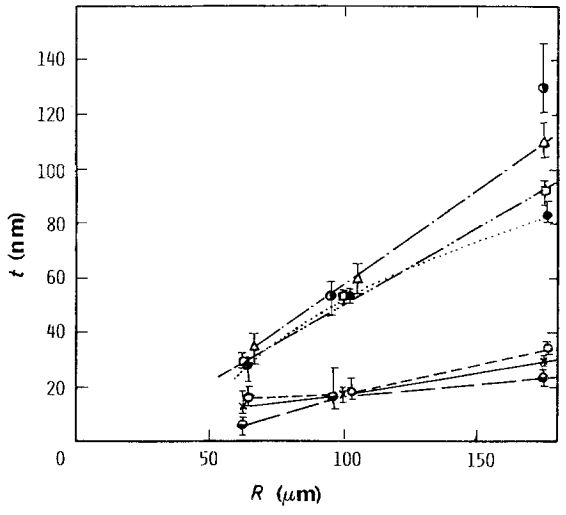

Figure 4 ZrO_2 coatings on fibres: thickness versus fibre radius. Coating solution, temperature (°C) and V (cm min^{-1}) as follows: (◑) C, 400, 32; (△) C, 200, 32; (◑) C, 200, 2.5; (×) D, 200, 2.5; (○) D, 800, 2.5; (□) D, 200, 19; (●) D, 800, 19.

TABLE III Coefficient n calculated from Equation 7 and average values of measured thickness

Solution	Heat treatment temperature (°C) (time = 3 min)	n		
		R = 62.5 μm	R = 100 μm	R = 175 μm
A	800	0.324	0.32	0.39
	400	–	0.32	0.22
B	800	0.51	0.52	0.73
	200	–	0.69	0.72
C	200	0.72	0.35	0.82
D	800	0.18	0.56	0.39
	200	0.35	0.54	0.59

the geometrical thickness. These results agreed well with those obtained from the scanning electron microscope.

The relationship between layer thickness and fibre radius is approximately linear as expressed by Equation 3. From Equation 2 it can be seeen that plotting the dimensionless thickness t/R against V should give a straight line passing through the origin. Fig. 5 shows a generally different trend, which could be explained by a non-Newtonian behaviour. The viscosity μ can be assumed [17] to be related to the shear rate γ by the equation

$$\mu(\gamma) = \frac{\mu}{\gamma^{1-n}} \quad (4)$$

For pseudo-plastic fluids the viscosity decreases with increasing shear rate ($n < 1$). The characteristic shear rate in the meniscus region during the coating operation is

$$\gamma = \frac{dV}{dy} = \frac{V}{h} \quad (5)$$

The dimensionless thickness h/R for a power-law liquid can be written in the form

$$\frac{h}{R} = L(n)\left(\frac{\mu}{\sigma}R^{1-n}V^{n}\right)^{2/(1+2n)} \quad (6)$$

where $L(n)$ is a constant dependent on n.

Equation 6 is identical to Equation 2 for $n = 1$ (Newtonian fluid). For constant R, constant solution properties and constant shrinkage it follows that

$$\frac{t}{R} = K' V^{2n/(1+2n)} \quad (7)$$

The n values were calculated from average experimental values of thickness t and are reported in Table III. The spread of values is very large, but n is less than unity for all cases, suggesting a non-Newtonian behaviour of the coating solutions used. However, both the determination of n and the dependence of n on R need more precise measurements.

4. Summary and conclusions

Silica glass fibres of three different diameters were coated with thin titania or zirconia layers by the dip-coating sol–gel method.

The coating thickness was measured by EPMA. A calibration curve was calculated by modelling of X-ray microanalysis based on multiple scattering theory using a Monte Carlo algorithm. EPMA measurement of coating thickness was verified on flat silica samples, coated with the same kind of layers used for fibres, by ellipsometry, optical reflectance, X-ray total reflection and by stylus apparatus. EPMA was demonstrated to be a suitable technique for the determination of layer thickness on curved surfaces.

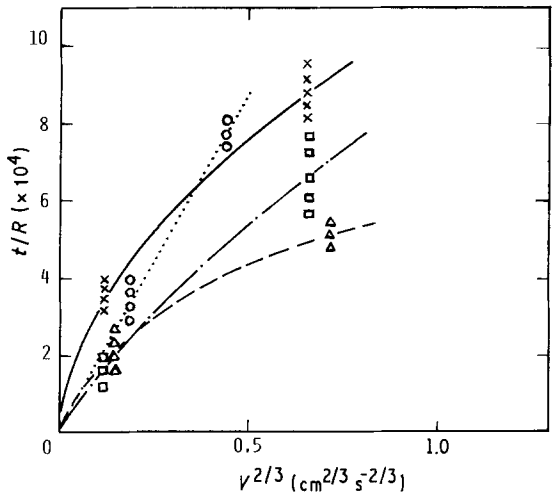

Figure 5 Dimensionless thickness t/R versus $V^{2/3}$ for solutions (×) A, (○) B, (□) C, (△) D.

Flat samples treated for 3 min at 500 °C were analysed by Raman spectroscopy and X-ray diffraction: anatase was detected in the titania layer.

The density of coatings was evaluated by the X-ray total reflection method on the above samples. Values of about 3.2 and 4.7 g cm^{-3} were found for TiO_2 and ZrO_2, respectively, indicating incomplete densification in both cases, in agreement with the low values of measured refractive indices.

The determined thicknesses of fibre coating were interpreted on the basis of theories developed for the dip-coating of fibres and for power-law fluids. A non-Newtonian behaviour of coating solutions was suggested.

References

1. T. BAAK, European Patent 0078749 (1982).
2. D. R. BISWAS and D. K. NATT, European Patent 0095728 (1983).

3. J. GÖTZ, H. MILOŠ, G. KUNKOVÁ and M. GUGLIELINI, Czech Patent 213–89 (1989).
4. K. JUREK, J. SIMSOVA and M. PAVLICEK, *Československý Časopis Pro Fyziku, Sekce A* **37** (1987) 146.
5. M. PAVLICEK, Research Report USP 459 (Prague, 1977).
6. R. M. A. AZZAM and N. M. BASHARA, "Ellipsometry and Polarized Light" (North-Holland, Amsterdam, 1977).
7. O. RENNER, *Czech. J. Phys. B* **22** (1972) 1007.
8. W. T. PAWLEWICZ, G. J. EXARHOS and W. E. CONAWAY, *Appl. Optics* **22** (1983) 1837.
9. L. S. SHU, C. Y. SHE and G. J. EXARHOS, *ibid.* **23** (1984) 3049.
10. L. S. HSU, R. SOLANKI, G. J. COLLINS and C. Y. SHE, *Appl. Phys. Lett.* **45** (1984) 1065.
11. I. STRAWBRIDGE and P. F. JAMES, *J. Non-Cryst. Solids* **82** (1986) 366.
12. H. SCHROEDER, *Phys. Thin Films* **5** (1969) 87.
13. B. E. YOLDAS and T. W. O'KEEFE, *Appl. Optics* **18** (1979) 3313.
14. I. STRAWBRIDGE and P. F. JAMES, *J. Non-Cryst. Solids* **86** (1986) 381.
15. M. GUGLIELMI and S. ZENEZINI, *ibid.* **121** (1990) 303.
16. J. A. TALLMADGE and D. A. WHITE, *I&EC Process Design & Devel.* **7** (1968) 503.
17. P. GROENVELD, *Chem. Eng. Sci.* **25** (1970) 1579.

Received 21 January
and accepted 7 June 1991